Field emission from dense, sparse, and patterned arrays of carbon nanofibers

K. B. K. Teo,[a] M. Chhowalla, G. A. J. Amaratunga, and W. I. Milne
Engineering Department, University of Cambridge, Trumpington Street, Cambridge CB2 1PZ, United Kingdom

G. Pirio, P. Legagneux, F. Wyczisk, and D. Pribat
Thales Research and Technology, Domaine de Corbeville, 91404 Orsay Cedex, France

D. G. Hasko
Microelectronics Research Centre, Cavendish Laboratory, University of Cambridge, Cambridge CB3 0HE, United Kingdom

(Received 27 November 2001; accepted for publication 29 January 2002)

We compare the field emission characteristics of dense (10^9 nanofibers/cm^2), sparse (10^7 nanofibers/cm^2), and patterned arrays (10^6 nanofibers/cm^2) of vertically aligned carbon nanofibers on silicon substrates. The carbon nanofibers were prepared using plasma-enhanced chemical vapor deposition of acetylene and ammonia gases in the presence of a nickel catalyst. We demonstrate how the density of carbon nanofibers can be varied by reducing the deposition yield through nickel interaction with a diffusion layer or by direct lithographic patterning of the nickel catalyst to precisely position each nanofiber. The patterned array of individual vertically aligned nanofibers had the most desirable field emission characteristics, highest apparent field enhancement factor, and emission site density. © *2002 American Institute of Physics.*
[DOI: 10.1063/1.1461868]

The remarkable field emission characteristics of carbon nanotubes/nanofibers have generated considerable interest in their application for vacuum microelectronic devices.[1–4] Due to their small diameters (few nanometers) and relatively long lengths (few microns), these high aspect ratio structures can generate a large electric field enhancement to obtain electron emission at low applied electric fields. Vertically aligned carbon nanotubes have been produced recently using various types of plasma-enhanced chemical vapor deposition (PECVD).[5–8] These nanotubes are perhaps the best candidates for field emission sources[9,10] because the alignment, precise position, height, and diameter of the structures can all be controlled.[6,11,12] The plasma grown nanotubes, which can be straight or conical depending on deposition parameters used,[8] structurally consist of tubular graphite walls with bamboo-type axial defects[6,8] and are also referred to as nanofibers in the literature.

High yield growth techniques such as chemical vapor deposition-based methods produce very dense arrays of nanotubes, and it is well known that electric field shielding effects from closely packed arrays of nanotubes adversely affect their field emission characteristics.[13,14] The authors in Refs. 13 and 14 reduced the nanotube density by lowering the concentration of a wet Fe-catalyst mixture which was used as the precursor for ''curly'' nonaligned nanotubes. We present results from vertically aligned nanofibers, whose density was controlled by using a barrier layer which reduced the nanofiber yield by interdiffusion with the catalyst. We were also able to fabricate and investigate the field emission properties of an ideal field emission array consisting of individual, vertically aligned nanofibers spaced twice their height apart to reduce the electric field shielding effect from adjacent nanofibers. Such an array of nanotubes/nanofibers has been previously conceived and theoretically investigated.[13,14] In this letter, we are able to experimentally confirm that this array exhibits lower turn-on fields and better overall field emission characteristics when compared with dense and sparse forests of ''randomly'' positioned vertically aligned nanofibers.

The vertically aligned carbon nanofibers were prepared on an *n*-doped Si substrate using dc-PECVD at 700 °C as described in Ref. 8. The catalyst used was a 3 nm thin film of Ni on a diffusion barrier layer (20 nm), both prepared by rf-magnetron sputtering. The diffusion barrier prevents the diffusion of Ni into Si at the growth temperature and typical barriers are insulating SiO_2 or conductive TiN.[15] The nanofiber growth was performed at 700 °C in the presence of acetylene and ammonia for 15 min. A −600 V bias was applied to the substrate to create the dc plasma. This process typically produces nanofibers which are $\sim 5\ \mu$m tall with a diameter of 50–100 nm.

The diffusion barrier can be used to determine the yield of nanofibers. Figure 1(a) shows the elemental depth profile of Ni on a TiN layer after annealing at 700 °C. Auger electron spectroscopy was used to examine the surface composition of the sample while a 2 keV Ar+ gun was used to sputter the surface layer-by-layer. We observed that the Ni clearly remained on the surface of the TiN which acted as a good barrier against diffusion during the annealing process. Deposition with a good diffusion barrier resulted in a high yield of densely packed nanofibers (10^9 nanofibers/cm^2) as shown in Fig. 2(a). If an ''imperfect'' diffusion barrier, such

[a]Author to whom correspondence should be addressed; electronic mail: kbkt2@eng.cam.ac.uk

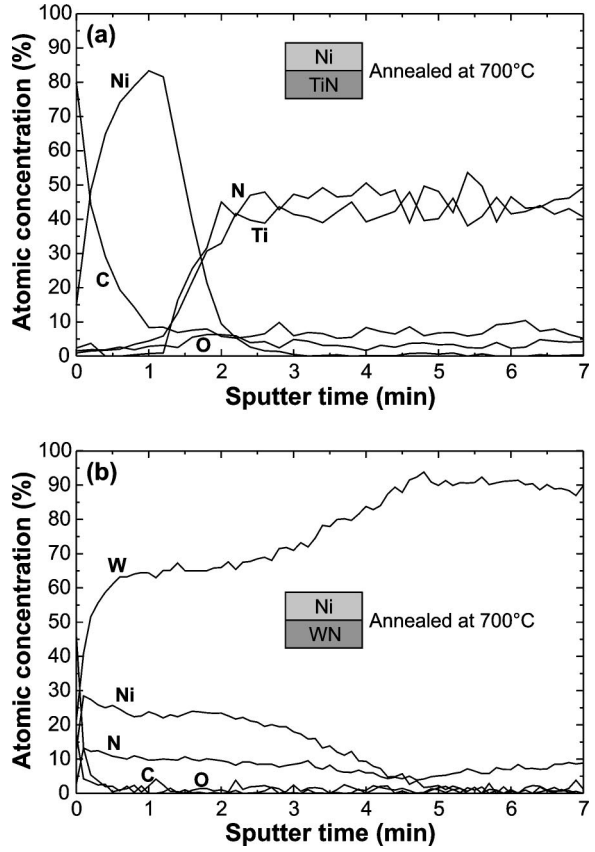

FIG. 1. Auger elemental composition of (a) Ni on TiN layer and (b) Ni on WN layer after annealing at 700 °C. An Ar ion gun was used to sputter the surface, and hence the sputter time (x axis) is related to the depth of the layer under investigation. The presence of C and O are probably due to chamber contaminants from the annealing process.

as tungsten nitride (WN) was used, the Ni diffused into the surface of the barrier at 700 °C [Fig. 1(b)] which left a small amount of Ni on the surface to catalyze nanofiber growth. Thus, deposition with a WN barrier layer produced a low yield of nanofibers which resembled a "sparse" forest of density 10^7 nanofibers/cm^2 [Fig. 2(b)]. The ordered array of single nanofibers in Fig. 2(c) was produced using electron beam lithography to pattern the catalyst such that individual freestanding nanofibers nucleated from each catalyst.[6,11,12] The nanofibers produced were $\sim 5\,\mu$m in height and

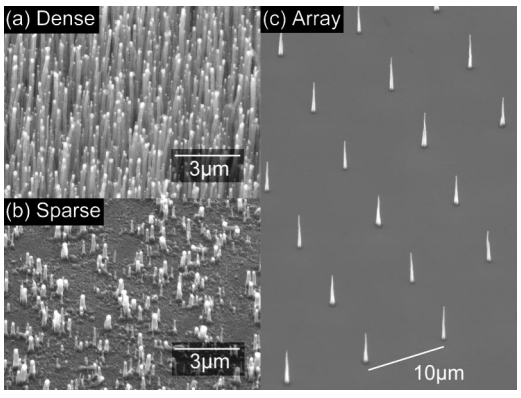

FIG. 2. (a) Densely packed forest of nanofibers containing 10^9 nanofibers/cm^2, (b) sparse forest of nanofibers containing 10^7 nanofibers/cm^2 and (c) an array of individual, vertically standing nanofibers spaced twice their height apart.

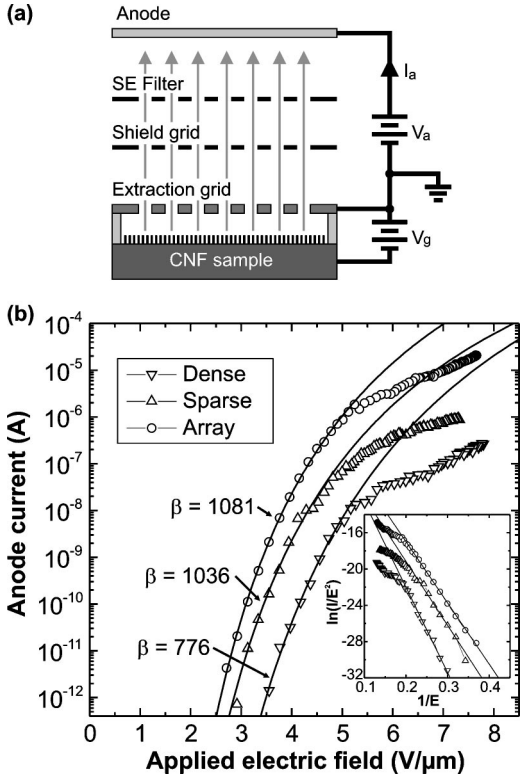

FIG. 3. (a) In the triode test setup, the grid voltage (V_g) is used to generate the extraction electric field, E, over the carbon nanofiber (CNF) sample for field emission. The test area is a 3 mm diameter circle and the physical grid transparency is 30%. (b) Field emission results from the dense forest, sparse forest, and array of nanofibers of Fig. 2. The solid curves are Fowler–Nordheim fits.

~ 55 nm in diameter. To reduce field shielding effects,[13,14] the nanofibers were spaced twice their height apart (10 μm). The spacing between the nanofibers essentially defined the density of the array to be 10^6 nanofibers/cm^2.

Field emission measurements were carried out on these samples using the hybrid triode assembly as shown in Fig. 3(a). A doped silicon grid was placed 100 μm away from the substrate to extract electrons which were then filtered for low energy secondary electrons (generated by electrons bombarding the silicon grid) before being collected by the anode placed 5 mm away. In the I–E characteristics of Fig. 3(b), we see that the patterned array of nanofibers exhibited the lowest turn-on field and highest anode current at any applied field. The sparse forest of nanofibers also exhibited significantly lower turn-on field and higher currents than the dense forest of nanofibers. Fowler–Nordheim (FN) fits were performed using the FN plot [inset Fig. 3(b)] using the current/field regions which do not show saturation. Assuming a work function of ~ 5 eV for the carbon nanofibers, the apparent field enhancement factors (β) of the patterned nanofiber array, sparse, and dense nanofiber forests were computed to be 1081, 1036, and 776, respectively. The error on the computed β is $\pm 2\%$. This result shows that the electric field shielding which occurs between closely packed nanofibers in the dense forest lowers the effective field enhancement factors of the high aspect ratio nanofibers. The sparse forest, to a certain extent, reduced the field shielding effects through lowering the density of nanofibers. The nanofibers of the sparse forest also had a large variation in height and diam-

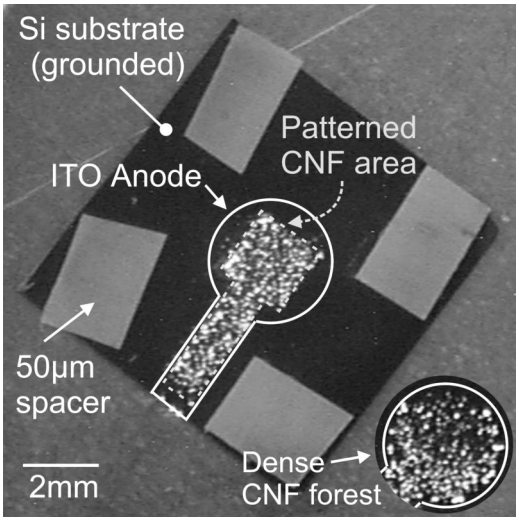

FIG. 4. Emission site density images of the patterned array of individual CNF and dense CNF forest (inset). The patterned array of nanofibers form the square keyhole inside the round keyhole which is the coated ITO anode area. The substrate and spacers can clearly be seen through the glass anode.

eter, and it is interesting that it exhibited a similar β as that of the patterned array. This implies that it is probably the higher aspect ratio structures in the sparse forest which are responsible for the majority of the emission current and the high β. Due to the random arrangement of the nanofibers in the sparse array, some field shielding still existed (as some nanofibers occurred in bunches) and the available substrate area was not optimally utilized. Hence, the sparse forest probably had a smaller total emission area, which resulted in lesser emission current as compared with the patterned array. With our hybrid triode assembly, current saturation was observed due to the triode geometry which used a thick ''100 um'' spacer and the transparency of the silicon grid. Electrons emitted with angles greater than ± 6 degrees are thus captured by the grid. The emission angle increases with the applied extraction field, causing an increased fraction of the emitted current to be captured by the grid. A more efficient triode geometry is to have an integrated grid.[9,10,16]

To test the current carrying capability and emission site density of the patterned array of nanofibers, we reverted to a simple diode structure where indium tin oxide (ITO) coated glass was used as the anode. The anode to sample spacing in this case was 50 μm. A field emission current of 1 mA (current density ~ 15 mA/cm^2) was obtained at an anode voltage of 700 V (~ 14 V/μm applied field). Luminescence was observed from the emitted electrons bombarding the ITO coated glass anode. As seen in Fig. 4, relatively high site density of at least 10^4 per cm^2 (resolution limited by CCD camera used) was achieved and the emission sites are indeed correlated to the patterned nanofiber area (square keyhole shape) under the ITO coated areas (large round keyhole shape) as indicated in Fig. 4. Note that emission site density of the nonpatterned dense CNF forest was an order less ($\sim 10^3$ per cm^2) and exhibited lesser uniformity. We also found that the emission site density of the patterned nanofiber array was 2 orders less than the nanofiber density of the array (10^6 per cm^2). This implies that although the nanofibers appeared uniform in height and diameter [Fig. 2(c)], the emission current from the nanofibers was not uniform over the whole area and only the nanofibers emitting sufficiently high currents produced an observable spot on the anode.

In conclusion, we have demonstrated that the density of carbon nanofibers can be decreased to enhance the field emission properties of vertically aligned carbon nanofiber emitters. A sparsely populated forest of nanofibers was produced by using a diffusion barrier such as WN to reduce the yield of nanofibers to 10^7 nanofibers per cm^2 from a normally very high yield (10^9 nanofibers per cm^2) Ni-catalyzed PECVD process. The field emission properties of the nanofibers were further optimized by using lithography to create an array of individual nanofiber emitters (10^6 nanofibers per cm^2), spaced twice their height apart to optimally reduce the electric field shielding from adjacent nanofibers. We find that although the nanofiber array had good height and diameter uniformity, realistically only a fraction of the emitters ($\sim 10^4$ per cm^2) were contributing significantly to the overall emission current from the array. This shows that small variations in the geometry of the nanofibers could cause large differences in the emission current, and the use of passive resistive ballast layers or active current control is necessary for obtaining more homogeneous emission over large areas.

This work was funded by the European Commission through the IST-FET project Nanolith and VA Tech Reyrolle. K.B.K.T. acknowledges the support from the Association of Commonwealth Universities and British Council.

[1] W. A. de Heer, A. Chatelaine, and D. Ugarte, Science **270**, 1179 (1995).
[2] P. G. Collins and A. Zettl, Appl. Phys. Lett. **69**, 1969 (1996).
[3] W. Zhu, C. Bower, O. Zhou, G. Kochanski, and S. Jin, Appl. Phys. Lett. **75**, 873 (1999).
[4] J. M. Kim, W. B. Choi, N. S. Lee, and J. E. Jung, Diamond Relat. Mater. **9**, 1184 (2000).
[5] Z. F. Ren, Z. P. Huang, J. W. Xu, J. H. Wang, P. Bush, M. P. Siegal, and P. N. Provencio, Science **282**, 1105 (1998).
[6] V. I. Merkulov, D. H. Lowndes, Y. Y. Wei, G. Eres, and E. Voelkl, Appl. Phys. Lett. **76**, 3555 (2000).
[7] C. Bower, W. Zhu, S. Jin, and O. Zhou, Appl. Phys. Lett. **77**, 830 (2000).
[8] M. Chhowalla, K. B. K. Teo, C. Ducati, N. L. Rupesinghe, G. A. J. Amaratunga, A. C. Ferrari, D. Roy, J. Robertson, and W. I. Milne, J. Appl. Phys. **90**, 5308 (2001).
[9] G. Pirio, P. Legagneux, D. Pribat, K. B. K. Teo, M. Chhowalla, G. A. J. Amaratunga, and W. I. Milne, Nanotechnology **13**, 1 (2002).
[10] M. A. Guillorn, A. V. Melechko, V. I. Merkulov, E. D. Ellis, C. L. Britton, M. L. Simpson, D. H. Lowndes, and L. R. Baylor, Appl. Phys. Lett. **79**, 3506 (2001).
[11] K. B. K. Teo, M. Chhowalla, G. A. J. Amaratunga, W. I. Milne, D. G. Hasko, G. Pirio, P. Legagneux, F. Wyczisk, and D. Pribat, Appl. Phys. Lett. **79**, 1534 (2001).
[12] K. B. K. Teo, G. Pirio, M. Chhowalla, S. B. Lee, P. Legagneux, D. G. Hasko, D. Pribat, H. Ahmed, G. A. J. Amaratunga, and W. I. Milne, Nanotechnology (submitted).
[13] L. Nilsson, O. Groening, C. Emmenegger, O. Kuettel, E. Schaller, L. Schlapbach, H. Kind, J. M. Bonard, and K. Kern, Appl. Phys. Lett. **76**, 2071 (2000).
[14] J. M. Bonard, N. Weiss, H. Kind, T. Stockli, L. Forro, K. Kern, and A. Chatelain, Adv. Mater. **13**, 184 (2001).
[15] A. M. Rao, D. Jacques, R. C. Haddon, W. Zhu, C. Bower, and S. Jin, Appl. Phys. Lett. **76**, 3813 (2000).
[16] C. A. Spindt, I. Brodie, L. Humphrey, and E. R. Westerberg, J. Appl. Phys. **47**, 5248 (1976).